Journal of Volcanology and Geothermal Research 347 (2017) 136–148

Contents lists available at ScienceDirect

Journal of Volcanology and Geothermal Research

journal homepage: www.elsevier.com/locate/jvolgeores

Geomorphology, lithofacies, and block characteristics to determine the origin, and mobility, of a debris avalanche deposit at Apacheta-Aguilucho Volcanic Complex (AAVC), northern Chile

Benigno Godoy [a,*], Inés Rodríguez [b,1], Marcela Pizarro [a,c], Germain Rivera [d]

[a] Centro de Excelencia en Geotermia de los Andes (CEGA), Departamento de Geología, Facultad de Ciencias Físicas y Matemáticas, Universidad de Chile, Plaza Ercilla 803, Santiago, Chile
[b] Departamento de Ciencias Geológicas, Facultad de Ingeniería y Ciencias Geológicas, Universidad Católica del Norte, Av. Angamos 0610, Antofagasta, Chile
[c] Departamento de Geología, Facultad de Ciencias Físicas y Matemáticas, Universidad de Chile, Plaza Ercilla 803, Santiago, Chile
[d] Enel Green Power Chile y Países Andinos, Av. Presidente Riesco 5335, Piso 14, Las Condes, Santiago, Chile

ARTICLE INFO

Article history:
Received 12 January 2017
Received in revised form 30 August 2017
Accepted 17 September 2017
Available online 19 September 2017

Keywords:
Apacheta-Aguilucho volcanic complex
Cerro Pabellon dome
Debris avalanche deposit
Hydrothermal alteration
Hummocks
Impact marks

ABSTRACT

Understanding the evolution of a volcanic edifice is important in establishing its associated geological hazards. Apacheta and Aguilucho volcanoes, northern Chile, formed a volcanic complex with known fumaroles and geothermal potential. Among the products resulting from the evolution of the Apacheta-Aguilucho Volcanic Complex (AAVC), a new volcanoclastic deposit has been recognized towards the eastern flank of the volcanic complex. This deposit is constituted by fragments of andesitic-to-dacitic lava and hydrothermally altered lava blocks. These fragments, which reach up to 5 m in diameter, form geomorphological structures such as hummocks, levées and ridges. Using these geomorphological characteristics, the distribution of the main lithological facies (or lithofacies), and fragment features (jigsaw cracks and impact marks), we proposed that this deposit was generated by a debris avalanche. This debris avalanche was triggered by partial collapse of an ancestral volcanic edifice occurred between 100 and 700 ka. The collapse of the AAVC ancestral edifice was influenced by hydrothermal alteration and the extensional tectonic setting that characterize the Cerro Pabellon Dome area. The mobility of the avalanche, and the genesis of the main geomorphological features associated with the deposit, are related to fragmentation of material during avalanche genesis and movement.

1. Introduction

Since the catastrophic eruption of Mt. St. Helens (May 18th, 1980), it have been established that partial collapse is a frequent process during evolution of a volcanic edifice (e.g. O'Callaghan and Francis, 1986; Belousov et al., 1999; van Wyk de Vries et al., 2001; Thouret et al., 2005; Carrasco-Nuñez et al., 2006; Ownby et al., 2007; Klemetti and Grunder, 2008). The collapse of a volcanic edifice produces a characteristic landslide type known as a debris avalanche. A debris avalanche (also named Sturzstroms; Hsü, 1975) is a stream of very rapidly moving debris derived from the disintegration of a fallen rock mass of large size (Hsü, 1975). Several mechanisms can trigger debris avalanches in volcanoes, such as: earthquakes (Keefer, 1984a, 1984b); magmatic intrusions (Voight, 2000); climate change (Capra, 2006); volcanic spreading (van Wyk de Vries and Francis, 1997; Cecchi et al., 2004); and, hydrothermal alteration (McGuire, 2003; Reid, 2004). The deposit generated by debris avalanche (hereafter named debris avalanche deposits) is a poorly sorted mixture of debris derived from the volcanic edifice (Ui, 1983; Siebert, 1984). Substrata material can be incorporated into the avalanche during its movement (Siebert, 1984; Ui et al., 2000).

Using remote sensing techniques (aerial photography and Landsat images) and field data, Francis and Wells (1988) recognized 14 major volcanic edifices with debris avalanche deposits in the Central Andes volcanic chain (14°–27°15′ S). These authors also observed that most of these deposits are very well preserved and oriented normal to the average strike of the main structures (NNE - SSW). Other authors have presented more detailed descriptions of the composition, morphology, mobility and origin of debris-avalanche deposits in the Central Andes (e.g. Francis et al., 1974; Francis et al., 1985; Naranjo and Francis, 1987; Wadge et al., 1995; van Wyk de Vries et al., 2001; Clavero et al., 2002; Richards and Villeneuve, 2001; Godoy et al., 2012; Rodríguez et al., 2015; Valderrama et al., 2016). These deposits are characterized by hummocky terrains and ridges structures, with some of these deposits also containing well-preserved levées.

In this paper we describe a new volcanoclastic deposit related with the evolution of the Apacheta-Aguilucho Volcanic Complex (AAVC), at northern Chile. This deposit presents a hummocky topography, with

* Corresponding author.
E-mail address: bgodoy@ing.uchile.cl (B. Godoy).
[1] Present address: Red Nacional de Vigilancia Volcánica, Servicio Nacional de Geología y Minería, Avenida Santa María 0104, Providencia, Santiago, Chile.

https://doi.org/10.1016/j.jvolgeores.2017.09.008
0377-0273/

hydrothermally altered blocks, and andesitic-to-dacitic lava fragments. The similar characteristics of deposits generated by debris-avalanche and glacial flows make it difficult to determinate the origin of such deposits. The aim of this paper is to define characteristics features of the new deposit discovered at AAVC. These features will be used to determine the origin of this deposit and to establish the dynamics of the flow.

2. Geological and structural setting

The Aguilucho and Apacheta volcanoes together form a volcanic complex (5557 m a.s.l.) located at 21°50′S and 68°10′W (Fig. 1). This complex is located in the Central Andes where volcanism is related to the subduction of the Nazca Plate beneath the South American Plate. The actual (<26 Ma) volcanic arc is located 250 km to 300 km from the Peru-Chile Trench, in a zone where the crustal thickness varies from 30 to 75 km (Allmendinger et al., 1997). This volcanic arc is represented mainly by calk-alkaline andesitic-to-dacitic lavas flows and ignimbrites (Lahsen, 1982; Scheuber and Giese, 1999; Trumbull et al., 2006; Salisbury et al., 2011), with some minor eruption of basaltic-andesite flows and dacitic domes (e.g. de Silva et al., 1994; Davidson and de Silva, 1995).

The AAVC is located in the southeastern limit of the Palpana-Inacaliri volcanic chain (Fig. 1). This chain trends NW-SE, parallel to the Calama-Olacapato-El Toro lineament (Salfity, 1985). The volcanic complex is composed of andesitic-to-rhyolitic lava flows, andesitic-to-dacitic pyroclastic flows and dacitic lava domes (Fig. 2; Ahumada and Mercado, 2009). Accordingly to Ramírez and Huete (1981), the basement has an Eocene-Miocene age and is made up of a sequence of andesitic lava flows, conglomerates, breccias, sandstones, limestones and gypsum. Over this basement, Miocene ignimbrites (7.5 Ma, Rivera et al., 2015) are exposed, while AAVC shows lava flows with ages of 700 ± 200 and 910 ± 140 ka (Rivera et al., 2015).

NW-striking normal faults are present from Inacaliri volcano to the AAVC (Tibaldi et al., 2009). The main fault system is called the Pabelloncito Graben and it is exposed towards the east of the volcanic complex (Fig. 2). In addition, the alteration of volcanic rocks, characterized by clay-silica sulfur mineral association, has been recognized on the W, E, NE and SW flanks of the AAVC (Urzua et al., 2002; Ahumada and Mercado, 2009; Fig. 2). This alteration is associated with fumarole activity present in the AAVC (Aguilera et al., 2008; Tassi et al., 2010).

3. Analytical techniques and study methods

Geomorphological structures (i.e. hummocks, ridges and levées) and their dimensions, lithological composition and description of block features, were carried out during field campaigns. Internal characteristics of the volcanoclastic deposit were difficult to recognize as only one road cuts the deposit (Fig. 3). Thus, only scarce internal characteristic on cross-cutting sections were observed. However, block features and lithological distribution were also recognized on the surface of geomorphological structures (Fig. 4).

Remote sensing (Landsat image, aerial photographies, and digital elevation models), and panoramic photographies were used to characterize the distribution of the geomorphological structures (Fig. 5), and different lithologies (Figs. 3,4) within the deposit.

4. Results

4.1. Deposit features

The studied volcanoclastic deposit (Unconsolidated Deposit; Fig. 2), has an area of ca. 3 km^2, and extends up to 4.5 km away from the eastern flank of the AAVC (Fig. 2). This deposit is mostly confined by two older andesitic-to-dacitic lava flows erupted during the first stage of the evolution of the volcanic complex (Ahumada and Mercado, 2009; Mercado et al., 2009) (Fig. 5b). The volcanoclastic deposit trends in an E-W direction, changing southeastward at the easternmost portion (Figs. 2, 5a).

During field campaigns, two main lithological facies (hereafter lithofacies) were characterized on the deposit (Figs. 3, 4): i) hydrothermal breccias., and ii) andesitic-to-dacitic lavas. The hydrothermal breccias lithofacies is composed of clay-rich hydrothermally altered lavas (Figs. 3a,b; 4a,b). The andesitic-to-dacitic lavas lithofacies range from fresh, light-to-dark grey, plagioclase-rich, vitreous andesite (Figs. 3b,c; 4c) to partially oxidized pyroxene-bearing dacite lava (Figs. 3c,4d). On the other hand, alluvial deposits were identified on the cross cutting section of the deposit (Fig. 3).

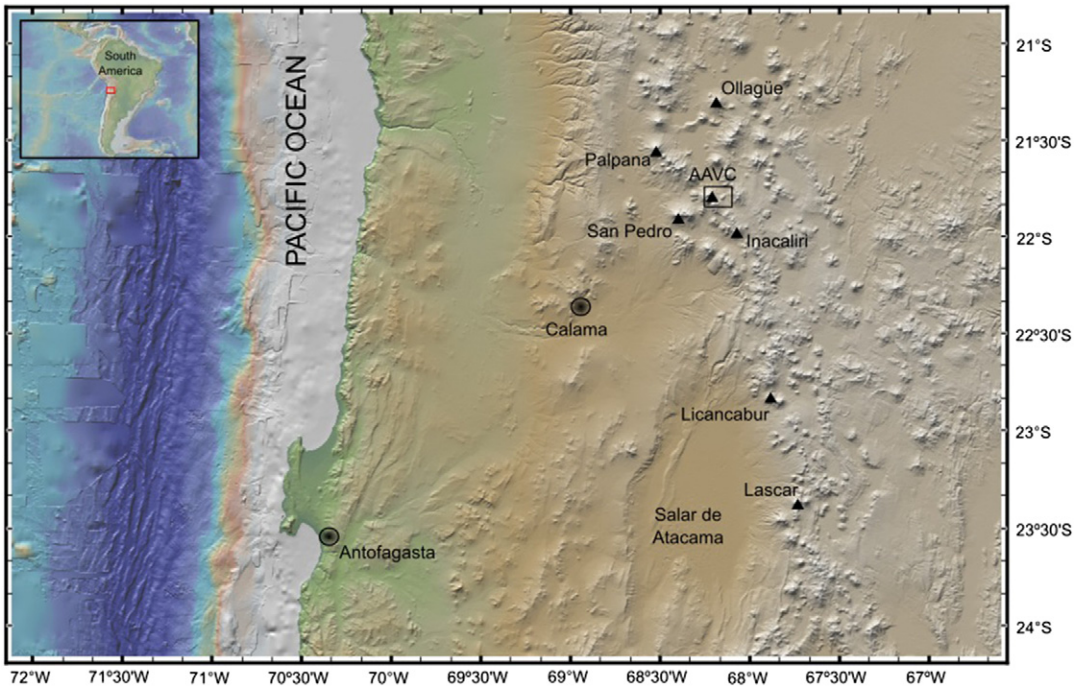

Fig. 1. Global Multi-Resolution Topography (GMRT) image showing the location of the Apacheta-Aguilucho Volcanic Complex (AAVC).

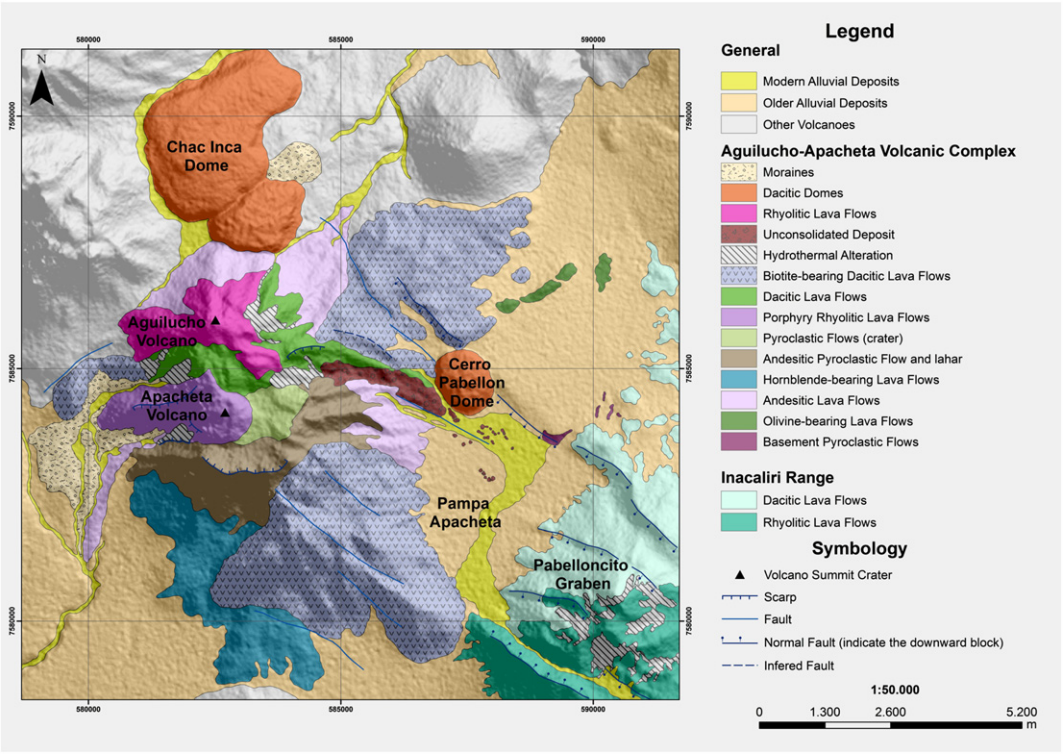

Fig. 2. Geological map of Apacheta-Aguilucho Volcanic Complex (AAVC) showing the main volcanic and structural features of the area (after Ahumada and Mercado, 2009). The deposit studied in this work is mapped as Unconsolidated Deposit to the west of the Cerro Pabellon Dome.

We use the terminology of Palmer et al. (1991) to describe individual components of this volcanoclastic deposit. Thus, according to the size of the fragments present, block and matrix were identified. Blocks are defined as fragments varying from 64 mm to 5 m diameter. The blocks are composed mainly by clast (64 mm–1 m length) and megaclast (>1 m length)(sensu Palmer et al., 1991) of the andesitic-to-dacitic lava lithofacies, although some blocks of the hydrothermal breccia lithofacies can be found scattered within the deposit (Figs. 3, 4). The blocks can present lithological homogeneity and brecciated textures (Figs. 3,4). Matrix refers to fragments with size <64 mm (pebble)(Figs. 3,4). In this deposit, the matrix corresponds mainly to interclast matrix (sensu Palmer et al., 1991) of hydrothermal breccias lithofacies surrounding blocks of andesitic-to-dacitic lavas lithofacies (Figs. 3b–c, 4c), with some intraclast matrix (sensu Palmer et al., 1991) present within blocks of the same composition (Figs. 3b–c, 4b).

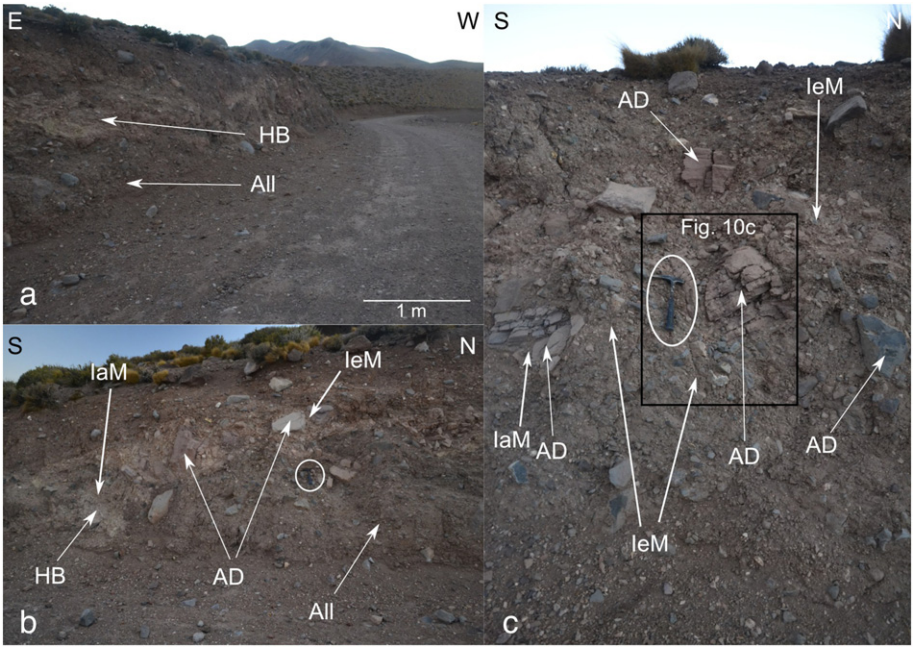

Fig. 3. Photographies of cross cutting sections of the volcanoclastic deposit at AAVC. Hydrothermal breccia (HB), and andesitic-to-dacitic (AD) blocks are recognized. Also, inter- (IeM), and intra-clast (IaM) matrix is shown. Alluvial deposits (All) are recognized below these sequences. In b) and c) circle with hammer as scale.

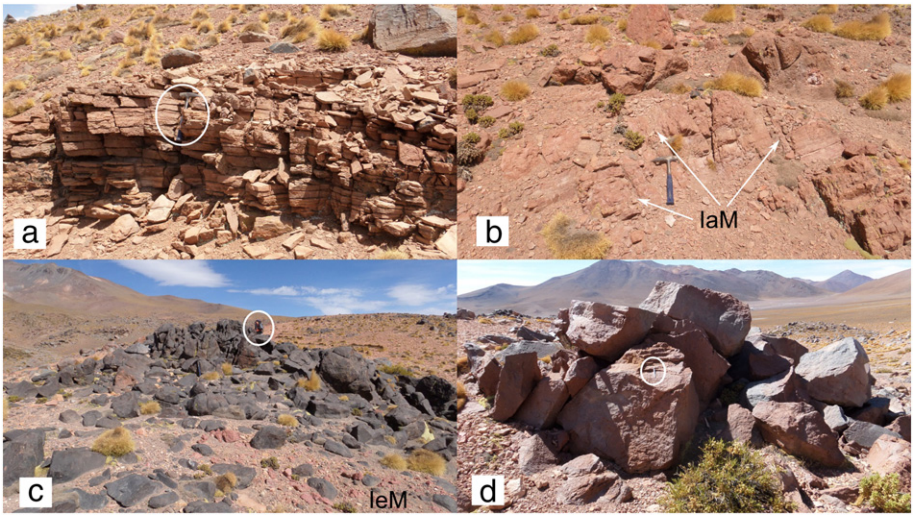

Fig. 4. Photographs of types of blocks found in the surface of geomorphologies at the deposit. a) Argillic andesite, and b) hydrothermal breccia. Hammer as scale. In b) intraclast matrix (IaM) is recognized. c) Vitreous plagioclase-rich andesite blocks (dark-grey) with hydrothermal breccia interclast matrix (IeM). Person as scale. d) Partially-oxidized dacitic blocks, with pen as scale.

Scattered striated blocks of andesitic-to-dacitic lava lithofacies were recognized within the deposit (Fig. 6a). Also, shattered blocks were observed at the surface, and within a few hummocks (Figs. 3, 4, 6b–c). Moreover, carved blocks were also recognized on the deposit (Fig. 6d–e).

4.2. Geomorphological characteristic of the deposit

Based on its geomorphological characteristics, this volcanoclastic deposit was divided into: a) a Main Unit with multiple tongue-shaped lobes; and, b) a flat plain with dispersed hummocks denominated Secondary Unit (Fig. 5a,c). The Main Unit, is constituted by hummocks, levées, and ridges (Fig. 7). Hummocks are composed mainly of andesitic-to-dacitic lava lithofacies towards the proximal areas (Fig. 8a–c), changing to hydrothermal breccia lithofacies, with scattered andesitic-to-dacitic lava lithofacies in the central portion of the volcanioclastic deposit (Fig. 8d–f): Levées (Fig. 9a–c) and ridges (Fig. 9d) are composed mainly of hydrothermal breccia lithofacies, and distribute to the marginal and distal zones of the Main Unit, respectively. This lithofacies distribution gives to the Main Unit its characteristic grey color in the middle, surrounded by pink color towards the border (Fig. 4d). At the proximal zone of the Main Unit, hummocks and levées are oriented almost on a E-W direction (Fig. 7), as described by Godoy et al. (2010). At the central and distal portions, hummocks and levées are mainly oriented NW-wards, while ridges are oriented on a E-W direction (Fig. 7)(Godoy et al., 2010). The Secondary Unit is comprised of small, scattered hummocks on a flat plain, near Cerro Pabellon Dome (Fig. 4b, 7). The isolated hummocks are composed mainly by andesitic-to-dacitic lava lithofacies (Fig. 10). These hummocks overlay a plain constituted by hydrothermal breccia lithofacies. Hummocks of

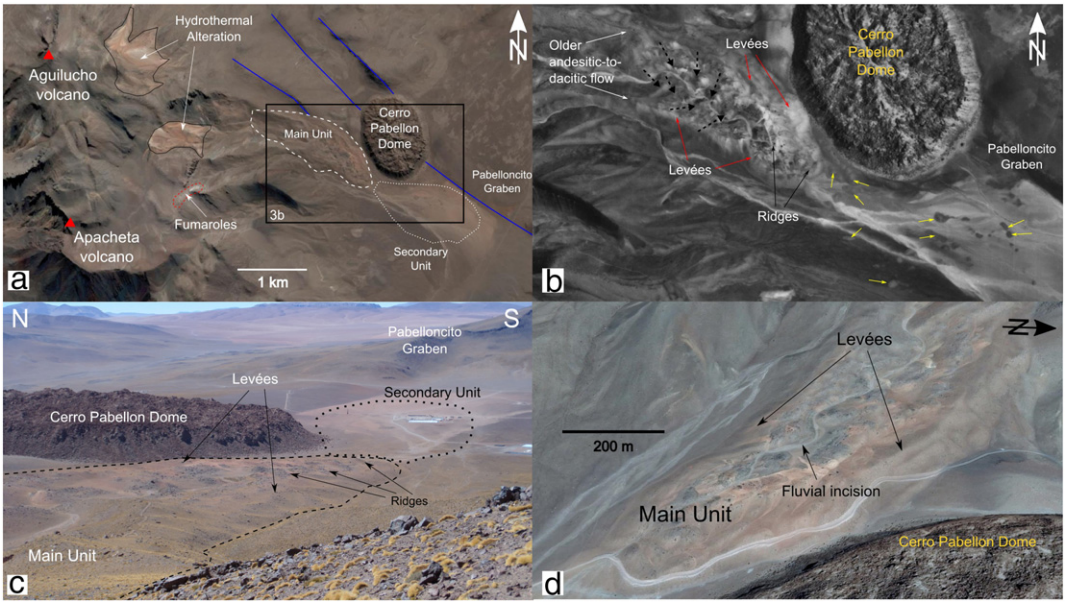

Fig. 5. Remote sensing used in this work. a) Ikonos satellite image (Google Earth™) showing main characteristics of AAVC. Blue lines correspond to normal faults associated to Pabelloncito Graben (after Ahumada and Mercado, 2009). b) Aerial photography showing detailed characteristic of the volcanoclastic deposit. Dashed arrows pointing to hummocks from the Main Unit. Small yellow arrows indicated scattered hummocks of the Secondary Unit. c) Panoramic photography, showing the two areas into which this deposit has been divided: Main (dashed fill) and Secondary (pointed fill) units. d) Ikonos satellite image (Google Earth™) showing the characteristic tongue-like shape of the Main Unit. Also, fluvial incision is recognized.

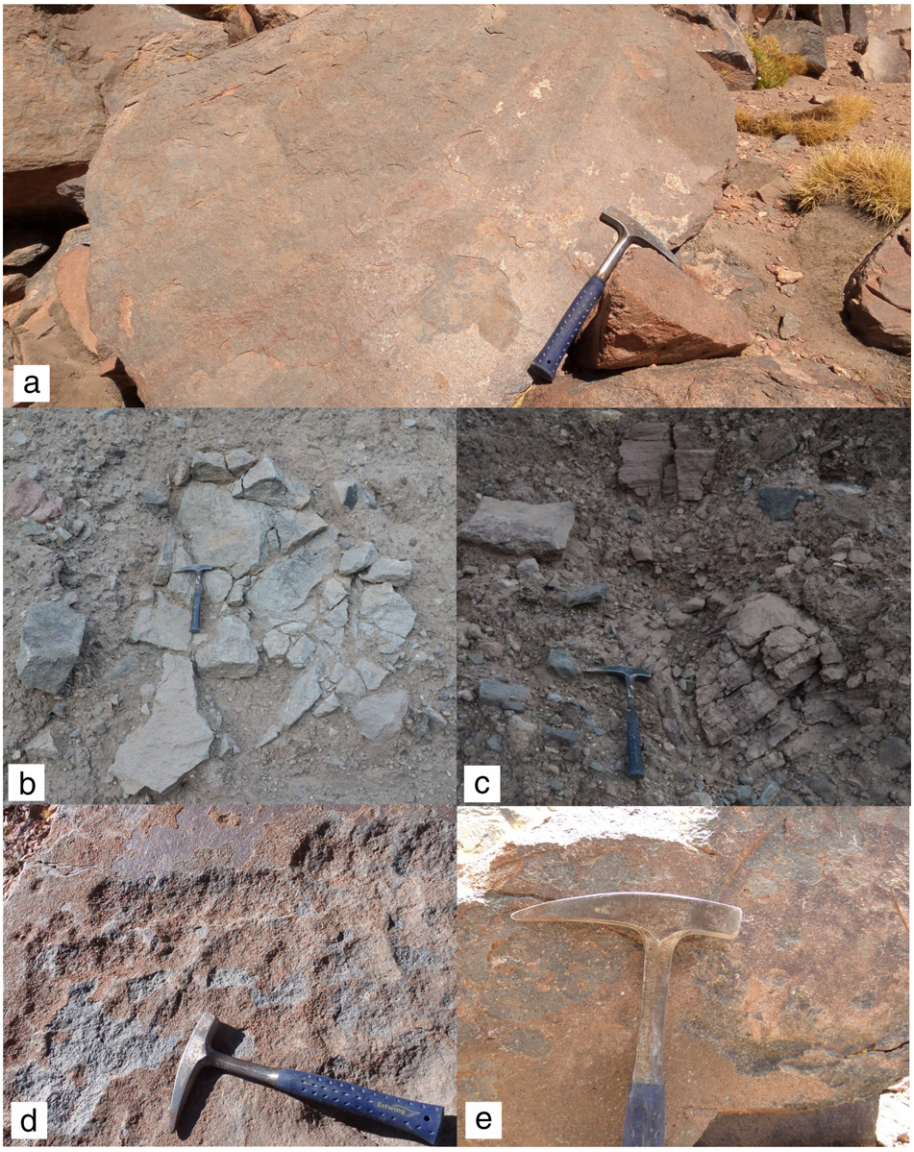

Fig. 6. Photographs of different blocks characteristics found in the deposit. a) Grooved block. b, c) Fragmented blocks. d, e) Carved blocks.

the Secondary Unit are oriented on a WNW direction (Fig. 7)(Godoy et al., 2010). For both units, the hummocks decrease in size with distance away from the volcano (Figs. 8, 10).

According to their characteristics, two types of hummocks have been identified: Type C, and Type B (sensu Glicken, 1996). Type C hummocks are composed mainly of blocks (>60% vol.) mixed with shattered matrix (sensu Glicken, 1996). These hummocks are recognized on the proximal zone of the Main Unit with heights between 5 and 30 m, a length up to 50 m, and megaclast reaching up to 5 m in diameter (Fig. 8a–c). Some stratified Type C hummocks are recognized within the deposit. These correspond to hummocks of andesitic-to-dacitic blocks overlying blocks and matrix of the hydrothermal breccia (Fig. 11). Type B hummocks are composed of both, matrix (>60% vol.) and blocks (<40% vol.). These hummocks are located towards the central and marginal zones of the Main Unit (Fig. 8d–f), and in the Secondary Unit of the deposit (Fig. 10). In the Main Unit Type B hummocks vary from 2 and 10 m height, reaching up to 20 m length, with megaclast up to 5 m in diameter (Fig. 8d–f). In the Secondary Unit, these hummocks have heights <2 m, lengths up to 50 m, and megaclast up to 2 m diameter (Fig. 10). Internal bedding or grading of the lithofacies within Type C and B hummocks was not observed.

Levées correspond to material distributed towards the northern and southern margins of the Main Unit (Fig. 9a–c). Levées are constituted by matrix of hydrothermal breccia lithofacies and scattered clast and megaclast of andesitic-to-dacitic lava lithofacies (Fig. 9a–c). Levées have heights up to 10 m, and extensions up to 900 m. Ridges are oriented on an E-W direction (Fig. 7), composed of scattered clast and megaclast of andesitic-to-dacitic lava lithofacies surrounded by matrix of hydrothermal breccia lithofacies (Fig. 9d). These structures have heights between 2 and 4 m, and lengths that vary between 10 and 20 m (Fig. 9d), reaching the furthest boundary of the Main Unit (Fig. 4).

5. Discussion

5.1. Origin of the volcanoclastic deposit

Although the hummocky topography observed in the volcanoclastic deposit recognized at the AAVC (Figs. 8,10) is typical for a debris-avalanche deposit (Ui, 1983, 1989; Ui et al., 2000), glacial deposits can also present hummocky morphology with moraines forming hummocks simply as product of supraglacial sedimentation (Johnson et al., 1995; Clayton et al., 2008; Bennett and Glasser, 2009). Moreover, leveés

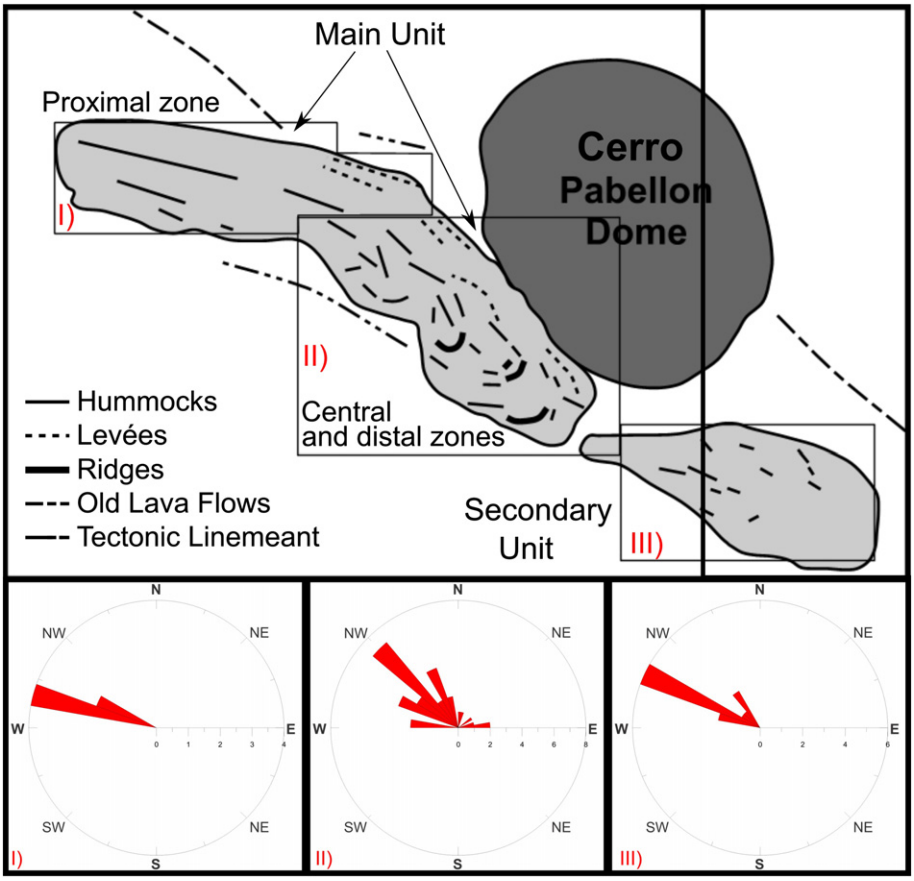

Fig. 7. Schematic representation of geomorphological structures (hummocks, levées and ridges) distributed at the deposit based on aerial photography form Fig. 5b (after Godoy et al., 2010). Rose diagrams show orientation of these structures on I) the proximal, and. II) central and distal zones of Main Unit, and. III) for hummocks of the Secondary Unit.

and ridges (Fig. 9) are characteristic of flow-developed mass movements (Dufresne and Davies, 2009; Valderrama et al., 2016). These geomorphological structures can be present on pyroclastic flows (e.g. Saucedo et al., 2002) and debris-avalanche deposits (Ui et al., 2000), being recognized on different volcanic edifices (e.g. Shasta, Crandell et al., 1984; Socompa, Wadge et al., 1995; Mount Saint Helens, Glicken, 1996; Parinacota, Clavero et al., 2002; Mombacho, Shea et al., 2008; Tutupaca, Valderrama et al., 2016). However, lateral and terminal moraines can generate morphologies similar to these structures (Fig. 12).

At the AAVC a steep, horseshoe-shape scar is facing towards the volcanoclastic deposit, which shows signs of strong hydrothermal alteration (Fig. 13). This hydrothermal alteration zone is covered by subsequently erupted volcanic material (Fig. 13). This volcanic material constitutes the crater of Aguilucho volcano and is composed of andesitic-to-dacitic pyroclastic and lava flows, with signs of moderated glacial erosion (Ahumada and Mercado, 2009). This indicates that the horseshoe-shape scarp morphology observed on the flank of the edifice was created either by failure of the volcanic edifice or by glacial erosion of the lavas, or both processes. Thus, internal characteristics (types, distribution and orientation of geomorphological structures, distribution of lithological facies, and blocks features), are useful in discriminating the origin of this volcanoclastic deposit (Ui, 1989).

5.1.1. Evidence for a non-glacial origin of the deposit

Glacial activity have been recognized on volcanoes of the Central Andes (e.g. San Pedro, O'Callaghan and Francis, 1986; Lascar, Gardeweg et al., 1998; Uturuncu, Sparks et al., 2008). Glacial features include U-shaped valleys, moraines and *roche moutonneé* (Gardeweg et al., 1998; Sparks et al., 2008). Glacial deposits are composed of unsorted and non-stratified material (Gutiérrez Elorza, 2008). These deposits can generate hummocky topography, with hummocks showing bedding and folding of incorporated material by stacking (Hambrey et al., 1997) or by till deformation below stagnated ice (Boone and Eyles, 2001).

At the deposit, isolated and scattered grooved blocks were observed (Fig. 6a). However, on the scarce cross-cutting sections found, it was not possible to observe folding or slumping, or internal bedding within hummocks. Moreover, a fluvial incision is recognized in the middle portion of the deposit (Fig. 5d). Fluvial incisions can be generated by glacial activity during melting (e.g. Moreau et al., 2005; Sahlin et al., 2009) (Fig. 12). On the other hand, similar incisions were observed on other flanks of the volcano. However, these incisions are not associated with hummocky terrain. Thus, we relate all the observed incisions to alluvial, and no to glacial events. Additionally, drumlins, glacio-lacustrine deposits, kamme, or other structures related to glacial activity have not been observed in this deposit.

Moreover, we have calculated the coefficient of friction for this volcanoclastic deposit with the formula from Ui (1983): $\Delta h/L$, where Δh is the difference between the maximum height related with the origin of the flow and the minimum height of the deposit; and, L is the maximum distance traveled by the flow from its origin. For this deposit Δh is 690 m and L is 4500 m, hence, the coefficient of friction is 0.15. This value is significantly lower than those between of 0.2 to 0.62 that represents deposits of glacial origin (Deline, 2009), and others from non-volcanic origin (Fig. 14) (Ui, 1983).

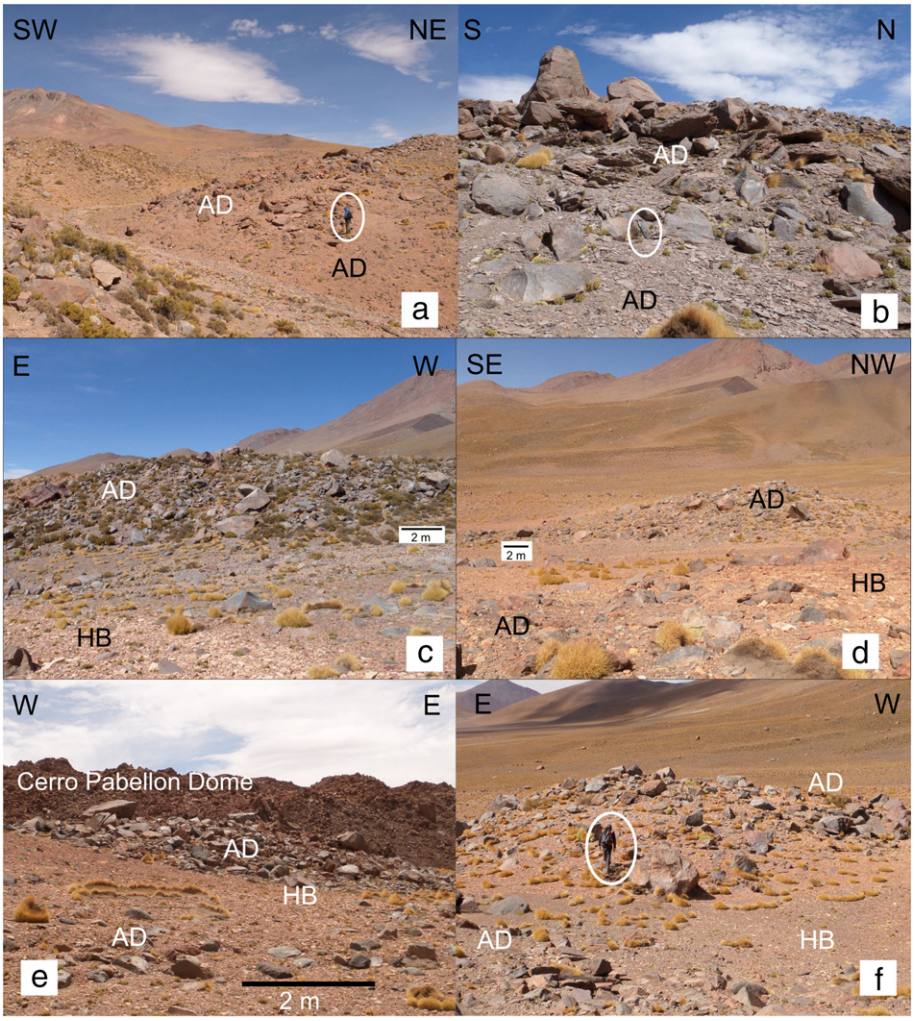

Fig. 8. Photographs of hummocks of the Main Unit, with recognized andesitic-to-dactic (AD) and hydrothermal breccia (HB) lithofacies. a), b) and c) proximal hummocks, with person (a), and hammer (b) as scale. These hummocks are mainly composed by AD fragments varying from 5 m to sand-sized diameter, and f) Hummocks of the central portion of the Main Unit constituted by AD blocks overlying HB fragments. On f) person as scale.

5.1.2. Debris-avalanche features of the deposit

Although present in various type of granular flows (Dufresne and Davies, 2009), hummocks, ridges, and levées are the main geomorphological features for debris avalanche deposits caused by partial collapse of volcanic edifices (Ui, 1983; Siebert, 1984; Ui et al., 2000; van Wyk de Vries and Delcamp, 2015). Moreover, partial collapse, and subsequent debris avalanche, is a common event during evolution of volcanoes at Central Andes (Francis and Wells, 1988).

It is common to observe volcano stratigraphic sequences undisrupted in hummocks and Toreva blocks in debris avalanche deposits (e.g. Palmer et al., 1991; Malone, 1995; Wadge et al., 1995; Kervyn et al., 2008; Godoy et al., 2012). Although no blocks with undisrupted stratigraphic sequences were observed at this deposit, the lithofacies distribution recognized in hummocks (Fig. 11) resembles the volcanic sequence exposed below the horseshoe-shaped lava flow at the eastern flank of the AAVC (Fig. 13). This volcanic sequence of hydrothermally altered lavas overlaying by andesitic-to-dacitic lava flows at the AAVC (Fig. 13) corresponds to the andesitic-to-dacitic lithofacies exposed over, and surrounded by, the hydrothermal breccia lithofacies observed in the deposit (Figs. 3, 4, 8, 11).

Also, debris avalanche deposits are characterized by spatial arrangement of block and matrix, and therefore hummocks types, across the deposit (Palmer et al., 1991; Takarada et al., 1999; Shea et al., 2008). This is related to the loosening and splitting of material which increase more fine-grained material to the distal area during debris avalanche advance (Ui et al., 1986). Type C hummocks in the proximal zone (Fig. 8a–c), correspond to the clast- and megaclast-rich debris avalanche zone, where blocks dominated (Palmer et al., 1991; Glicken, 1996). Towards distal areas, the hummocks are enriched of matrix (Type B hummocks; Figs. 8d–f, 9 and 10), corresponding to the matrix-rich debris avalanche (Palmer et al., 1991; Glicken, 1996).

The observed progressive decrease in size of hummocks towards distal zones is another characteristic of debris-avalanche deposits (e.g. Takarada et al., 1999; Clavero et al., 2002; Voight et al., 2002; Shea et al., 2008; Godoy et al., 2012). This feature is related to a process that occurs during avalanche mobility, related to avalanche dynamics (see below).

The presence of jigsaw puzzle-type fractures - or jigsaw cracks (Fig.6b,c), and carved features, known as impact marks (Fig. 6d,e), on blocks within hummocks are another evidence that this deposit was generated by a debris avalanche. Jigsaw cracks correspond to shattered blocks generate by breaking of the avalanche material (Ui et al., 1986; Glicken, 1996). During the avalanche movement the blocks disaggregate, thus jigsaw cracks are more common closer to the source zone (Ui et al., 1986; Glicken, 1996). Impact marks are related to small-scale collision between fragments during avalanche movement

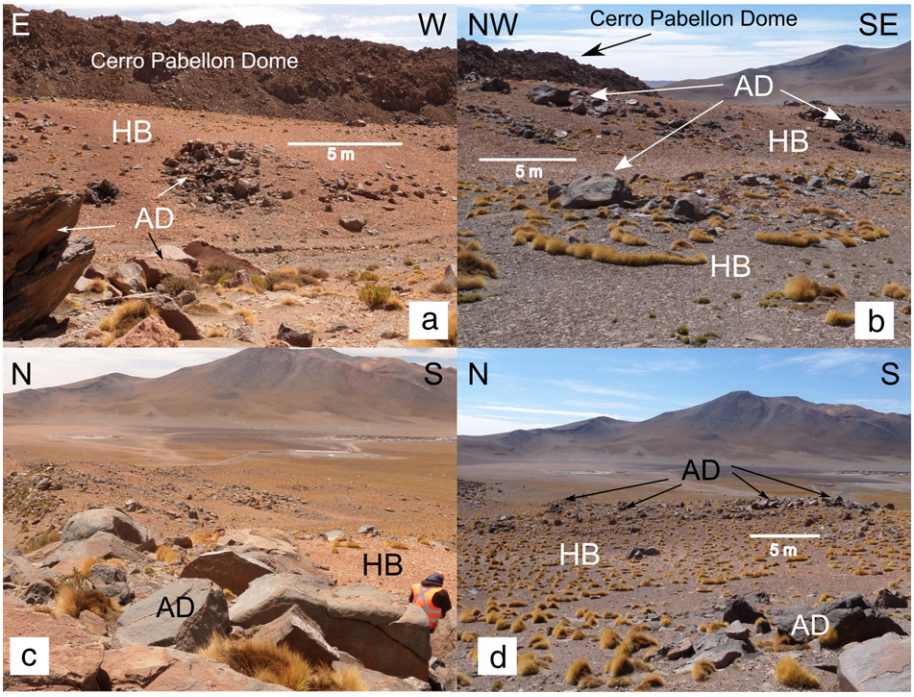

Fig. 9. Photographs of levees from the northern (a,b), and southern (c) margins of the deposit, and from a transversal ridge (d) recognized in the Main Unit. These structures are composed of andesitic-to-dacitic (AD) and hydrothermal breccia fragments (HB).

(Clavero et al., 2002). Impact marks had been observed in debris avalanche deposits of Parinacota (Clavero et al., 2002), Llullaillaco (Rodríguez et al., 2009), and Irruputuncu (Bacigalupo et al., 2015) volcanoes at Central Andes.

Moreover, the calculated coefficient of friction for this volcanoclastic (0.15) is akin with avalanche deposits at other volcanoes in the Central Andes (e.g. Lastarria, Páez et al., 2015; Llullaillaco, Rodríguez et al., 2009; Socompa, Wadge et al., 1995) (Fig. 14).

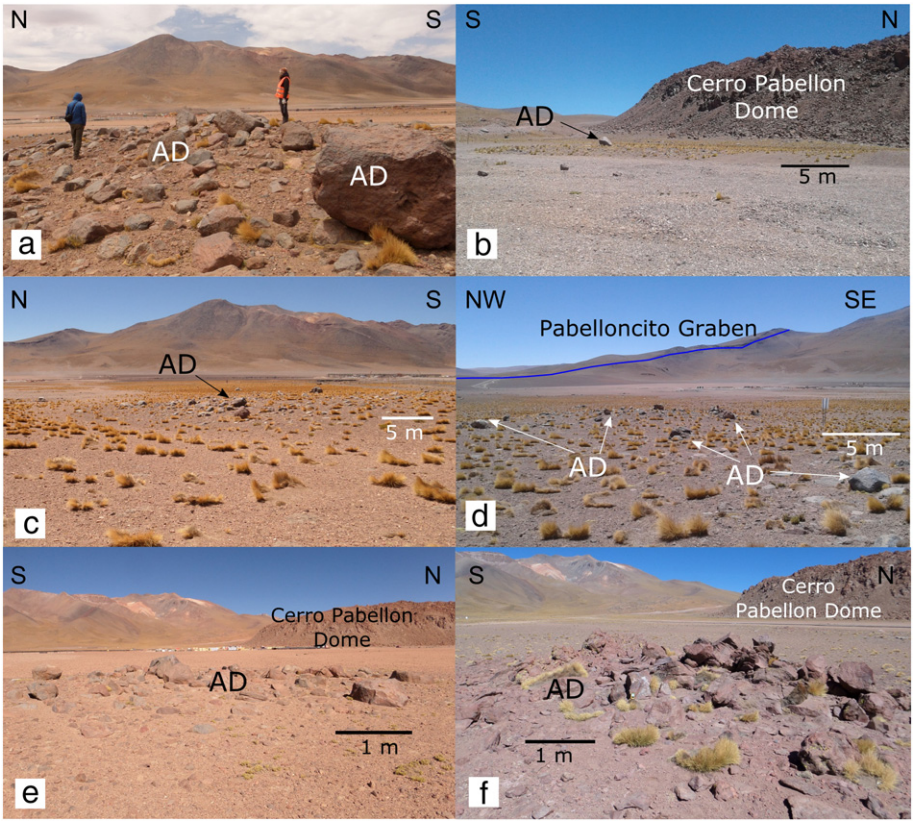

Fig. 10. Photographs of geomorphological features of the Secondary Unit. Isolated hummocks present blocks (>64 mm) of andesitic-to-dacitic lithofacies (AD) scattered on finer grained fragments.

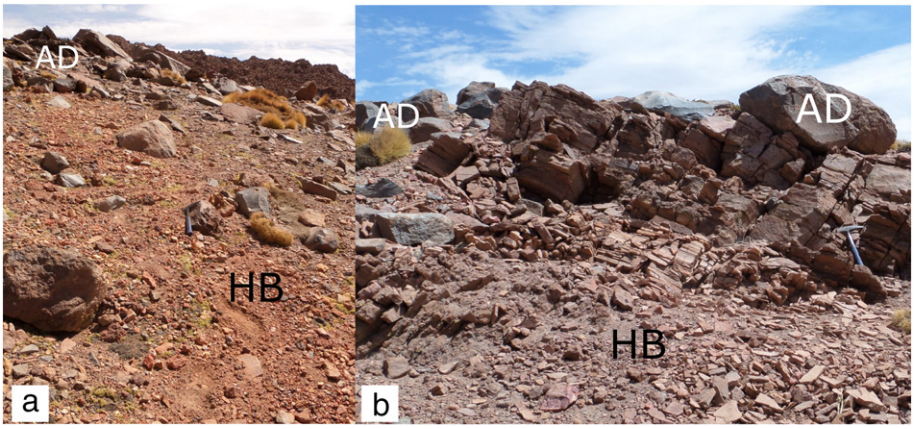

Fig. 11. Photographs of internal bedding observed at hummocks occurring between hydrothermal breccia (HB) block and matrix, and andesitic-to-dacitic lava (AD) blocks.

Thus, considering all the characteristics, a debris-avalanche as opposed to glacial origin is proposed for the volcanoclastic deposit distributed on the eastern flank of the AAVC.

5.2. Cause of the volcanic collapse

Several mechanisms that trigger volcano edifice collapse have been proposed, with the most important being: substrata spreading; magmatic intrusions; fault reactivation beneath volcanic edifices; and, hydrothermal alteration (Voight et al., 1981; van Wyk de Vries et al., 2000, 2001; Voight, 2000; McGuire, 2003; Reid, 2004; Wooller et al., 2009). At AAVC, no pyroclastic deposits are associated to this debris-avalanche deposit. This eliminates magmatic activity as a triggering mechanism of edifice collapse. In addition, no folding, slumping, or bulldozer-type structures were found in the deposit, making it unlikely that edifice collapse was caused by spreading of volcanic substrata (McGuire, 1996; van Wyk de Vries and Francis, 1997; Cecchi et al., 2004).

Clay-rich hydrothermally altered lava is recognized within the deposit (Figs. 3 and 4) and in the avalanche scar (Fig. 13). Hydrothermal altered material weakens the rocks of the volcanic edifice making it plausible for collapse (van Wyk de Vries et al., 2000; Cecchi et al., 2004). In the case of the AAVC, hydrothermal alteration is linked to fumarolic activity present at the summit of the volcanic complex (Urzua et al., 2002; Aguilera et al., 2008; Ahumada and Mercado, 2009). This suggests that hydrothermal alteration of the main edifice played an important role on volcano stability.

Moreover, the local tectonic setting and regional structures can also play important roles in the collapse of volcanic edifices (Merle et al., 2006; Carrasco-Nuñez et al., 2006; Wooller et al., 2009). For the Central Andes, Francis and Wells (1988) established that almost all of the studied debris-avalanche deposits show a relationship with the main tectonic setting of the region: sector collapses show a strong tendency to occur oriented perpendicular to the regional fault trend. In the Inacaliri-Palpana volcanic chain, NW-SE striking structures are the main structural system (Fig. 2). According to Tibaldi et al. (2009) the Inacaliri-Palpana volcanic chain is located in an extensional regime since the Late Miocene, indicated by the presence of normal faults in the Pabelloncito Graben (Fig. 2) (Ahumada and Mercado, 2009). In the AAVC, the avalanche scar is oriented almost normal to the NW-SE treding Pabelloncito Graben. Hence, the reactivation of this fault system and the combination with hydrothermal alteration could have triggered the collapse of the volcanic edifice.

Dating the volcanic units of AAVC gave an age of 0.7 ± 0.2 and 0.91 ± 0.14 Ma (Mercado et al., 2009; Rivera et al., 2015), while Cerro Pabellon Dome has an estimated age of ~100 ka (Renzulli et al., 2006; Tierney et al., 2016). As no runout of the avalanche exists over Cerro Pabellon Dome, we suggest that the deposit was generated before the eruption of this dome, but it is younger than the last dated flow of the volcano.

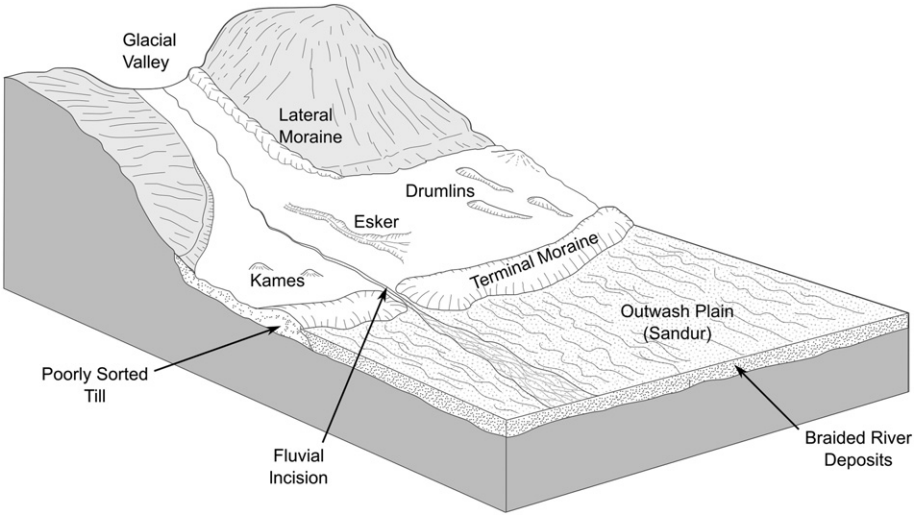

Fig. 12. Schematic representation of glacial landforms and glacial deposits in continental glaciated areas (after Nichols, 2009). Terminal moraines can be associated with ridge geomorphology, while the form of lateral moraine resembles that of levées. Also, fluvial incision by melting of the glacier is recognized.

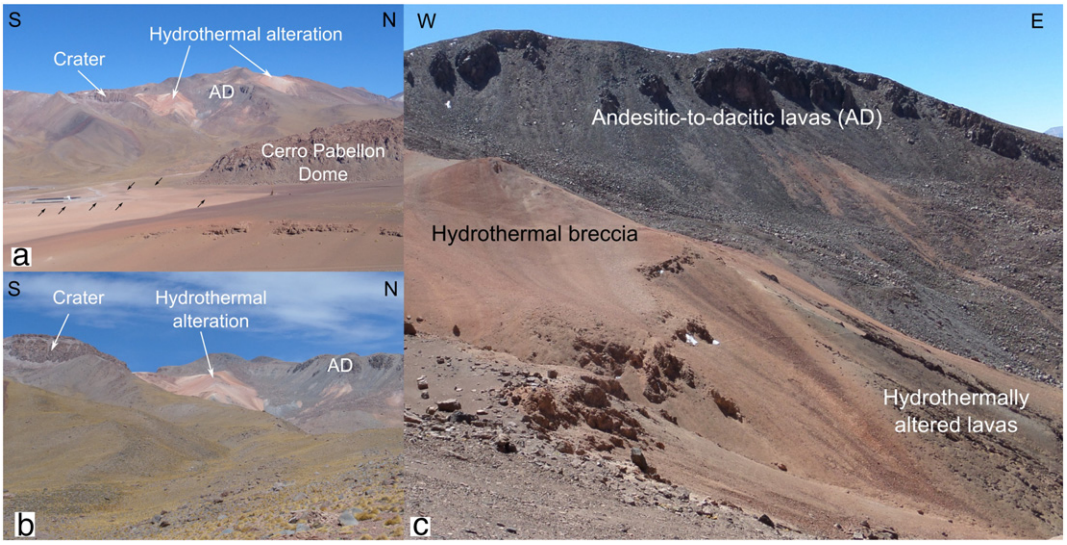

Fig. 13. Photographs of the Apacheta-Aguilucho volcanic complex showing the horseshoe-shaped scar morphology, and lithologies recognized at the eastern flank of the volcanic complex. The photographs show hydrothermal alteration and a crater composed of dacitic pyroclastic and lava flows (Ahumada and Mercado, 2009) as part of the volcano. Also, andesitic-to-dacitic lavas (AD) cropping out above hydrothermal alteration can be observed. On a) arrows point to scattered hummocks of the Secondary Unit. On c) sequence of the main lithologies at the top of the volcanic complex is observed.

5.3. Avalanche dynamics

The orientation of hummocks, including those generating ridges, and leveés gives hint of the flow direction during avalanche movement (e.g. Siebert, 1984; Wadge et al., 1995; Shea et al., 2008; Dufresne and Davies, 2009). Using aerial photographies (Fig. 5b), Godoy et al. (2010) proposed that the location and orientation of hummocks, leveés and ridges of the proximal, central, and distal zones of the Main Unit, and hummocks from the Secondary Unit are linked to the mobility of the avalanche during its flow (Fig. 7). Thus, at edifice collapse, the resulting avalanche flowed in an east-west direction (Godoy et al., 2010). This is confirmed by the orientation of proximal hummocks and levees of the Main Unit (Fig. 7). The avalanche maintained this flow direction until it encountered older lava flows exposed on the eastern side of the volcanic complex. These lava flows channeled and deflected the avalanche flow towards a NW-SE direction (Fig. 7). This generated hummocks and levées parallel to flow direction, and ridges oriented almost normal to this direction in the central and distal zones of the Main Unit (Fig. 7). In the terminal zone (i.e. Secondary Unit) the flow moved unconfined in a WNW-ESE orientation (Godoy et al., 2010).

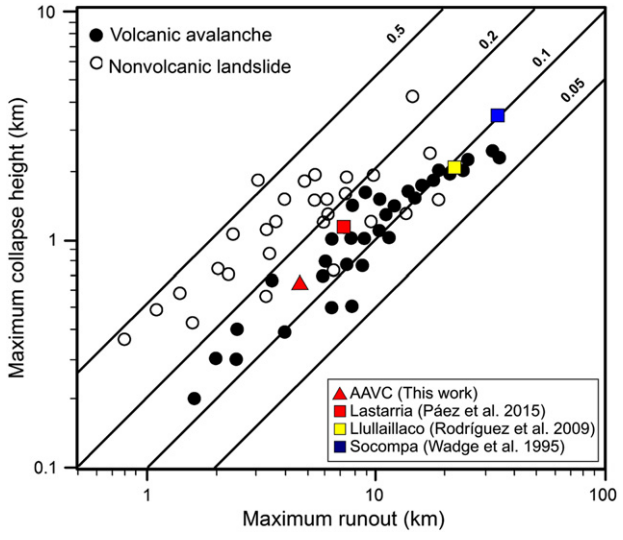

Fig. 14. Diagram showing the coefficients of friction of the deposit related to another volcanic and non-volcanic deposits (after Ui, 1983). Data from Socompa (Wadge et al., 1995), Llullaillaco (Rodríguez et al., 2009), and Lastarria (Páez et al., 2015) are included.

In the scarce hummocks cut by new roads, the deposit shows no liquefaction or deformation structures (Fig. 3). This indicates that material traveled with little deformation as domains (sensu Clavero et al., 2002), and entrainment of unconsolidated material was not the main mechanism of mobility as observed in other debris avalanche deposits (e.g. Clavero et al., 2002, 2004; Hungr and Evans, 2004). Fragmentation of a debris avalanche into domains is a consequence of loose surface blocks that continued their movement forward, as the avalanche comes to rest (e.g. Clavero et al., 2002). Davies and McSaveney (2002, 2009) suggested that fragmentation of landslides are responsible for their large run-out. Experimentally, these authors conclude that fragmentation decreases shear stress at the base of the flow. Thus, fragmentation causes extension and spreading of the material during its movement downward from the volcanic edifice (Davies and McSaveney, 2002, 2009. Fig. 15). This explains the characteristics of Type C hummocks in the proximal zone of the deposit, the generation of Type B hummocks towards marginal and distal zones, and the large distance traveled by the scattered blocks of andesitic-to-dacitic lava lithofacies distributed in the Secondary Unit (Fig. 15). Fragmentation also explains the decreasing size of hummocks as the avalanche moves away from its source (e.g. Takarada et al., 1999; Clavero et al., 2002; Shea et al., 2008).

Thus, a granular movement caused by fragmentation of the avalanche material is proposed. Besides the aforementioned hummocks and blocks characteristics, granular flow also explains the presence of longitudinal levees and transversal ridges in the deposit. Leveés are common features of granular flows emplaced into narrow valleys, by flow interaction with the dry, sloping valley walls (Dufresne and Davies, 2009). Generation of levées in this volcanoclastic deposit is related by the confinement of the avalanche by two older andesitic-to-dacitic lava flows (Fig. 5b). Moreover, transversal ridges are also generated by granular flows (Dufresne and Davies, 2009). These transversal ridges are generated by compression of the material due deceleration (Dufresne and Davies, 2009; Roberti et al., 2017) (Fig. 15). Hence, we suggest that the presence of transversal ridges towards the distal zone of the depositwas caused by deceleration of the avalanche by changes on paleotopographic conditions during its movement (Fig. 15).

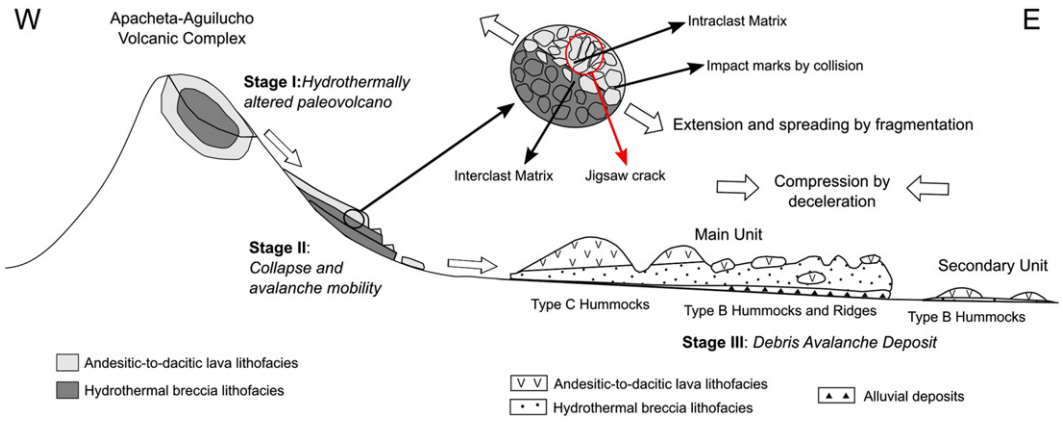

Fig. 15. a) Schematic representation of the Debris Avalanche Deposit (Stage III) with distribution of main lithofacies and different types of hummocks. This representation also shows the distribution of material before collapse of the ancestral edifice (Stage I), where the innermost part is constituted by hydrothermally altered material surrounded of fresher andesitic-to-dacitic lithologies. The mobility of the avalanche was trigged by spreading through fragmentation of the avalanche material (Stage II). Schematic distribution of lithologies on Stage I according to the present exposure of lavas and hydrothermal alteration at the eastern flank of the volcano observed in Fig. 12.

Moreover, the presence of impact marks present on blocks within the hummocks is another indicator of granular flow of debris avalanche. The impact marks on blocks (Fig. 6), and intraclast matrix (Figs. 3–4) were generated by granular collision during flow. Thus, a granular movement is responsible for the dynamics of the debris avalanche at the AAVC (Fig. 13).

5.4. Paleovolcano distribution

The preservation of the stratigraphic sequence of a debris-avalanche deposit can be used to determine the distribution of material in the volcano prior to its collapse (e.g. Godoy et al., 2012). For El Crater debris-avalanche deposit, Shea et al. (2008) proposed that the wide distribution of hydrothermal breccia fragments within the deposit indicated that this material corresponds to the innermost fraction of the collapsed paleovolcano. Moreover, for Tutupaca volcano, Valderrama et al. (2016) recognized that the hydrothermally altered lavas constituting the lower unit, and the unaltered dome fragments corresponding to the upper unit of the debris-avalanche deposit defined the position of material at the volcano prior to its eruption. In this deposit, the undisrupted stratigraphic distribution of hydrothermally altered blocks under andesitic-to-dacitic lava fragments (Fig. 11), the presence of andesitic-to-dacitic lava fragments surrounded by hydrothermal breccias (Figs. 4,8–9), and the distribution of Type C and Type B hummocks (Fig. 15), suggest that andesite-to-dacite fragments were distributed above the hydrothermally altered material before the volcanic collapse (Fig. 15). Also, the wide distribution of hydrothermal breccia fragments towards the central, distal, and marginal portion of the deposit (Fig. 8–9) suggests that this material corresponds to the innermost fraction of the collapsed paleovolcano (Fig. 15). Therefore, the alteration due to hydrothermal activity in the paleovolcano progressively decreased from the core outwards in the volcanic edifice. This is similar to the present state of the eastern flank of the AAVC, with scarce signs of alteration in the most external lava flows, (Fig. 13).

6. Conclusions

Aguilucho and Apacheta volcanoes constitute a volcanic complex located in the Central Andes. Towards its eastern flank, this volcanic complex shows hummocky topography and other distinctive geomorphological structures. Using field descriptions and remote sensing, this paper performs a new characterization of a debris avalanche deposit. This deposit has a tongue-like morphology (Main Unit), with scattered hummocks (Secondary Unit) towards its distal zone. The deposit covers an area of ca. 3 km^2, with a length of 4.5 km. This deposit is made up of two main lithological facies: andesitic-to-dacitic lavas, and hydrothermal breccias. Also, two types of hummocks were identified and described: Type C hummocks which are predominantly made of andesitic-to-dacitic blocks (64 mm–5 m) with shattered matrix (<64 mm) of andesitic-to-dacitic intraclast and hydrothermal breccia interclast; and, Type B hummocks which are predominantly composed of hydrothermal breccia matrix, and scattered andesitic-to-dacitic blocks.

Although scarce, internal features, together with hummocks, levees and ridges characteristics, and jigsaw cracks and impact marks present on blocks at this volcanoclastic deposit of the AAVC indicate a debris avalanche origin. This avalanche was generated by partial collapse of the ancestral volcano caused by hydrothermally altered material that weakened the volcanic edifice. This collapse was also influenced by tectonic characteristic of the volcano, considering that the AAVC is located in the downward block of the Pabelloncito Graben, related with the present extension on the Cerro Pabellon dome area.

Previous work established an initial movement of the avalanche on an E-W orientation. This movement changes to NW-SE, ending on a WNW-ESE orientation towards the distal zones. We propose that this movement was controlled by fragmentation of material during avalanche progress.

Based on relations with dated units, we estimated the age of the deposit as older than 100 ka, but younger than 700 ka. However, active fumaroles observed at the AVVC, and the presence of fault structures related to the existing tectonic regime of the area could result in another collapse of one sector of the present volcano.

Acknowledgments

Authors thank Dr. Lucia Capra and an anonymous reviewer for helpful comments. We thank Dr. Felipe Aguilera (Universidad Católica del Norte), Sergio Ahumada, and José Luis Mercado for discussions on early versions of this manuscript. We also thank Dr. Santiago Maza, Dr. (c) Estefania Camus, M.Sc. (c) Bernardita Alvear, and Camila Lizana (Universidad de Chile), and Dr. (c) Marco Taussi (University of Urbino, Italy) for their help during field campaigns. Dr. Petrus Le Roux and Dr. Chris Harris (University of Cape Town, South Africa) contributed on improvement of previous versions of this manuscript. This work was funded by CONICYT-FONDAP Project n° 15090013. Marcela Pizarro is funded by a PhD grant from CONICYT-PCHA/Doctorado Nacional n° 2014-21240597. Benigno Godoy is funded by FONDECYT PostDoctoral Project n° 3160432. We thank Enel Green Power Chile for logistic accommodations.

References

Aguilera, F., Ahumada, S., Mercado, J.L., Piscaglia, F., Renzulli, A., Tassi, F., 2008. Geological Survey, Petrology and Gas Geochemistry of the Apacheta-Aguilucho Volcanoes (Andean Central Volcanic Zone, Northern Chile) and their Related Geothermal System. *In* Congresso del Gruppo Nazionale di Geofisica Della Terra Solida. Trieste, Italy.

Ahumada, S., Mercado, J.L., 2009. Evolucióno geológica y estructural del complejo volcánico Apacheta-Aguilucho (CVAA), Segunda Región, Chile. *Dissertation*, Bachelor's Degree Thesis, Universidad Católica del Norte. Chile, Antofagasta.

Allmendinger, R.W., Jordan, T.E., Kay, S.M., Isacks, B., 1997. The evolution of the Altiplano-Puna plateau of the Central Andes. Annu. Rev. Earth Planet. Sci. 25 (1):139–174. https://doi.org/10.1146/annurev.earth.25.1.139.

Bacigalupo, C., Rodríguez, I., Campos, E., 2015. Mecanismos de emplazamiento de la avalancha de detritos del volcán Irruputuncu, Andes Centrales. *In* Actas XIV Congreso Geológico Chileno, La Serena, Chile. 3, pp. 57–60.

Belousov, A., Belousova, M., Voight, B., 1999. Multiple edifice failures, debris avalanches and associated eruptions in the Holocene history of Shiveluch volcano, Kamchatka, Russia. Bull. Volcanol. 61 (5):324–342. https://doi.org/10.1007/s004450050300.

Bennett, M., Glasser, N., 2009. Glacial Geology: Ice Sheets and Landforms. 2nd edition. John Wiley and Sons Ltd, West Sussex, United Kingdom (385 pp).

Boone, S.J., Eyles, N., 2001. Geotechnical model for great plains hummocky moraine formed by till deformation below stagnant ice. Geomorphology 38 (1–2):109–124. https://doi.org/10.1016/S0169-555X(00)00072-6.

Capra, L., 2006. Abrupt climatic changes as triggering mechanisms of massive volcanic collapses. J. Volcanol. Geotherm. Res. 155 (3–4):329–333. https://doi.org/10.1016/j.jvolgeores.2006.04.009.

Carrasco-Nuñez, G., Díaz-Castellón, R., Siebert, L., Hubbard, B., Sheridan, M.F., Rodríguez, S.R., 2006. Multiple edifice-collapse events in the Eastern Mexican Volcanic Belt: the role of sloping substrate and implications for hazard assessment. J. Volcanol. Geotherm. Res. 158 (1–2):151–176. https://doi.org/10.1016/j.jvolgeores.2006.04.025.

Cecchi, E., van Wyk de Vries, B., Lavest, J.-M., 2004. Flank spreading and collapse of weak-cored volcanoes. Bull. Volcanol. 67 (1):72–91. https://doi.org/10.1007/s00445-004-0369-3.

Clavero, J.E., Sparks, R.S.J., Huppert, H.E., Dade, W.B., 2002. Geological constraints on the emplacement mechanism of the Parinacota debris avalanche, northern Chile. Bull. Volcanol. 64 (1):40–54. https://doi.org/10.1007/s00445-001-0183-0.

Clavero, J., Polanco, E., Godoy, E., Aguilar, G., Sparks, R.S.J., van Wyk de Vries, B., Pérez de Arce, C., Matthews, S., 2004. Substrata influence in the transport and emplacement mechanism of the Ollagüe debris avalanche (northern Chile). Acta Vulcanol. 16 (1–2), 59–76.

Clayton, L., Attig, J.W., Ham, N.R., Johnson, M.D., Jennings, C.E., Syverson, K.M., 2008. Ice-walled-lake plains: implications for the origin of hummocky glacial topography in middle North America. Geomorphology 97 (1–2):237–248. https://doi.org/10.1016/j.geomorph.2007.02.045.

Crandell, D.R., Miller, C.D., Glicken, H.X., Christiansen, R.L., Newhall, C.G., 1984. Catastrophic debris avalanche from ancestral Mount Shasta volcano, California. Geology 12 (3):143–146. https://doi.org/10.1130/0091-7613.

Davidson, J.P., de Silva, S.L., 1995. Late Cenozoic magmatism of the Bolivian Altiplano. Contrib. Mineral. Petrol. 119 (4):387–408. https://doi.org/10.1007/BF00286937.

Davies, T.R.H., McSaveney, M.J., 2002. Dynamic simulation of the motion of fragmenting rock avalanches. Can. Geotech. J. 39 (4), 789–798.

Davies, T.R., McSaveney, M.J., 2009. The role of rock fragmentation in the motion of large landslides. In: Bonnard, C., Laloui, L., Scavia, C., Castelli, M. (Eds.), The Mechanics and Velocity of Large Landslides. Engineering Geology 109:pp. 67–79. https://doi.org/10.1016/j.enggeo.2008.11.004.

Deline, P., 2009. Interactions between rock avalanches and glaciers in the Mont Blanc massif during the late Holocene. Quat. Sci. Rev. 28 (11—12):1070–1083. https://doi.org/10.1016/j.quascirev.2008.09.025.

Dufresne, A., Davies, T.R., 2009. Longitudinal ridges in mass movement deposits. Geomorphology 105 (3–4):171–181. https://doi.org/10.1016/j.geomorph.2008.09.009.

Francis, P.W., Wells, G.L., 1988. Landsat thematic mapper observations of debris avalanche deposits in the Central Andes. Bull. Volcanol. 50 (4):258–278. https://doi.org/10.1007/BF01047488.

Francis, P.W., Roobol, M.J., Walker, G.P.L., Cobbold, P.R., Coward, M., 1974. The San Pedro and San Pablo volcanoes of northern Chile and their hot avalanche deposits. Geol. Rundsch. 63 (1):357–388. https://doi.org/10.1007/BF01820994.

Francis, P.W., Gardeweg, M., Ramirez, C.F., Rothery, D.A., 1985. Catastrophic debris avalanche deposit of Socompa volcano, northern Chile. Geology 13 (9):600–603. https://doi.org/10.1130/0091-7613.

Gardeweg, M.C., Sparks, R.S.J., Matthews, S.J., 1998. Evolution of Lascar Volcano, Northern Chile. London]–>J. Geol. Soc. Lond. 155 (1):89–104. https://doi.org/10.1144/gsjgs.155.1.0089.

Glicken, H., 1996. Rockslide-debris avalanche of May 18, 1980, Mount St. Helens Volcano, Washington. Open-file report n°96-677. US Geol. Surv. (90 pp).

Godoy, B., Aguilera, F., Ahumada, S., Mercado, J., 2010. Flow direction of debris avalanche at Aguilucho-Apacheta Volcanic Complex (AAVC), Central Andes. In American Geophysical Union, Fall Meeting 2010, Abstract #NH51C-1239, San Francisco, CA, USA.

Godoy, B., Clavero, J., Rojas, C., Godoy, E., 2012. Facies volcánicas del depósito de avalancha de detritos del volcán Tata Sabaya, Andes Centrales. Andean Geol. 39 (3):394–406. https://doi.org/10.5027/andgeoV39n3-a03.

Gutiérrez Elorza, M., 2008. Geomorfología. Pearson Educación, S.A., Madrid, España (920 pp).

Hambrey, M.J., Huddart, D., Bennett, M.R., Glasser, N.F., 1997. Genesis of 'hummocky moraines' by thrusting in glacier ice: evidence from Svalbard and Britain. London]–>J. Geol. Soc. Lond. 154 (4):623–632. https://doi.org/10.1144/gsjgs.154.4.0623.

Hsü, T., 1975. Catastrophic debris streams (Sturzstroms) generated by rockfalls. Geol. Soc. Am. Bull. 86 (1):129–140. https://doi.org/10.1130/0016-7606.

Hungr, O., Evans, S.G., 2004. Entrainment of debris in rock avalanches: an analysis of a long run-out mechanism. Geol. Soc. Am. Bull. 116 (9/10):1240–1252. https://doi.org/10.1130/B25362.1.

Johnson, M.D., Mickelson, D.M., Clayton, L., Attig, J.W., 1995. Composition and genesis of glacial hummocks, western Wisconsin, USA. Boreas 24 (2):97–116. https://doi.org/10.1111/j.1502-3885.1995.tb00630.x.

Keefer, D.K., 1984a. Landslides caused by earthquakes. Geol. Soc. Am. Bull. 95 (4):406–421. https://doi.org/10.1130/0016-7606.

Keefer, D.K., 1984b. Rock avalanches caused by earthquakes: source characteristics. Science 223 (4642):1288–1290. https://doi.org/10.1126/science.223.4642.1288.

Kervyn, M., Klaudius, J., Keller, J., Mbede, E., Jacobs, P., Ernst, G.G.J., 2008. Remote sensing study of sector collapses and debris-avalanche deposits at Oldoinyo Lengai and Kerimasi volcanoes, Tanzania. Int. J. Remote Sens. 29 (22):6565–6595. https://doi.org/10.1080/01431160802168137.

Klemetti, E.W., Grunder, A.L., 2008. Volcanic evolution of Volcán Aucanquilcha: a long-lived dacite volcano in the Central Andes of northern Chile. Bull. Volcanol. 70 (5):633–650. https://doi.org/10.1007/s00445-007-0158-x.

Lahsen, A., 1982. Upper Cenozoic volcanism and tectonism in the Andes of northern Chile. Earth Sci. Rev. 18 (3–4):285–302. https://doi.org/10.1016/0012-8252(82)90041-1.

Malone, D.H., 1995. Very large debris-avalanche deposit within the Eocene volcanic succession of the northeastern Absaroka Range, Wyoming. Geology 23 (7):661–664. https://doi.org/10.1130/0091-7613.

McGuire, W.J., 1996. Volcano instability: a review of contemporary themes. In: McGuire, W.J., Jones, A.P., Neuberg, J. (Eds.), Volcano Instability on the Earth and other Planets. Geological Society, London, Special Publication. 110:pp. 1–23. https://doi.org/10.1144/GSL.SP.1996.110.01.01.

McGuire, W.J., 2003. Volcano instability and lateral collapse. Theol. Rev. 1, 33–45.

Mercado, J.L., Ahumada, S., Aguilera, F., Medina, E., Renzulli, A., Piscaglia, F., 2009. Geological and structural evolution of Apacheta-Aguilucho Volcanic Complex (AAVC), Northern Chile. In Actas XII Congreso Geológico Chileno, Santiago, Chile (S7:002).

Merle, O., Barde-Cabusson, S., Maury, R.C., Legendre, C., Guille, G., Blais, S., 2006. Volcano core collapse triggered by regional faulting. J. Volcanol. Geotherm. Res. 158 (3–4):269–280. https://doi.org/10.1016/j.jvolgeores.2006.06.002.

Moreau, J., Ghienne, J.-F., Le Heron, D.P., Rubino, J.-L., Deynoux, M., 2005. 44 Ma ice stream in North Africa. Geology 33 (9):753–756. https://doi.org/10.1130/G21782.1.

Naranjo, J.A., Francis, P., 1987. High velocity debris avalanche at Lastarria volcano in the north Chilean Andes. Bull. Volcanol. 49 (2):509–514. https://doi.org/10.1007/BF01245476.

Nichols, G., 2009. Sedimentology and Stratigraphy. 2nd Edition. John Wiley & Sons Ltd, The Atrium, Southern Gate, Chichester, West Sussex, United Kingdom 419 pp.

O'Callaghan, L.J., Francis, P.W., 1986. Volcanological and petrological evolution of San Pedro volcano, Provincia El Loa, North Chile. J. Geol. Soc. Lond. 143 (2):275–286. https://doi.org/10.1144/gsjgs.143.2.0275.

Ownby, S., Delgado Granados, H., Lange, R.A., Hall, C.M., 2007. Volcán Tancítaro, Michoacán, Mexico, 40Ar/39Ar constraints on its history of sector collapse. J. Volcanol. Geotherm. Res. 161 (1–2):1–14. https://doi.org/10.1016/j.jvolgeores.2006.10.009.

Páez, J., Campos, E., Rodríguez, I., 2015. Análisis de la avalancha de detritos del volcán Lastarria, Andes Centrales: facies, parámetros físicos y dinámica. In Actas XIV Congreso Geológico Chileno, La Serena, Chile. 3, pp. 15–18.

Palmer, B.A., Alloway, B.V., Neall, V.E., 1991. Volcanic-debris-avalanche deposits in New Zealand – lithofacies organization in unconfined, wet-avalanche flows. Sedimentation in Volcanic Settings, Society for Sedimentary Geology Special Publication. 45, pp. 89–98.

Ramírez, C., Huete, C., 1981. Carta Geológica de Chile, Hoja Ollagüe. Escala 1: 250.000. Carta n°40. Instituto de Investigaciones Geológicas, Santiago, Chile.

Reid, M.E., 2004. Massive collapse of volcano edifices triggered by hydrothermal pressurization. Geology 32 (5):373–376. https://doi.org/10.1130/G20300.1.

Renzulli, A., Menna, M., Tibaldi, A., Flude, S., 2006. New data of surface geology, petrology and Ar-Ar geochronology of the Altiplano-Puna Volcanic Complex (northern Chile) in the framework of future geothermal exploration. In Actas XI Congreso Geologico Chileno, Antofagasta, Chile. 2, pp. 307–310.

Richards, J., Villeneuve, M., 2004. Erratum to: The Llullaillaco volcano, northwest Argentina: construction by Pleistocene volcanism and destruction by sector collapse. J. Volcanol. Geotherm. Res. 105 (4):77–105. https://doi.org/10.1016/S0377-0273(03)00430-X.

Rivera, G., Morata, D., Ramírez, C., 2015. Evolución vulcanolíga y tectónica del área del Cordón Volcánico Cerro del Azufre – Cerro Inacaliri y su relación con el sistema geotérmico de Pampa Apacheta, II Región de Antofagasta, Chile. In Actas XIV Congreso Geológico Chileno, La Serena, Chile, pp. 556–559.

Roberti, G., Friele, P., van Wyk de Vries, B., Ward, B., Clague, J.J., Perotti, L., Giardino, M., 2017. Rheological evolution of the Mount Meager 2010 debris avalanche, southwestern British Columbia. Geosphere 13 (2). https://doi.org/10.1130/GES01389.1 (14 p.).

Rodríguez, I., Clavero, J., Arancibia, G., Godoy, E., Rojas, C., 2009. Estudio de facies y análisis de parámetros físicos del depósito de avalancha de detritos del Volcán Llullaillaco, Andes Centrales. In Actas XII Congreso Geológico Chileno, Santiago, Chile (S2:012).

Rodríguez, I., Roche, O., Moune, S., Aguilera, F., Campos, E., Pizarro, M., 2015. Evolution of Irruputuncu volcano, Central Andes, northern Chile. J. S. Am. Earth Sci. 63:385–399. https://doi.org/10.1016/j.jsames.2015.08.012.

Sahlin, E.A.U., Glasser, N.F., Jansson, K.N., Hambrey, M.J., 2009. Connectivity analyses of valley patterns indicate preservation of a preglacial fluvial valley system in the Dyfi basin, Wales. Proc. Geol. Assoc. 120 (4):245–255. https://doi.org/10.1016/j.pgeola.2009.10.001.

Salfity, J.A., 1985. Lineamientos transversales al rumbo andino en el noroeste Argentino. In Actas IV Congreso Geológico Chileno, Antofagasta, Chile. 2, pp. 119–137.
Salisbury, M.J., Jicha, B.R., de Silva, S.L., Singer, B.S., Jiménez, N.C., Ort, M.H., 2011. $^{40}Ar/^{39}Ar$ chronostratigraphy of Altiplano-Puna volcanic complex ignimbrites reveals the development of a major magmatic province. Geol. Soc. Am. Bull. 123 (5/6):821–840. https://doi.org/10.1130/B30280.1.
Saucedo, R., Macías, J.L., Bursik, M.I., Mora, J.C., Gavilanes, J.C., Cortes, A., 2002. Emplacement of pyroclastic flows during the 1998–1999 eruption of Volcán de Colima, México. J. Volcanol. Geotherm. Res. 117 (1–2):129–153. https://doi.org/10.1016/S0377-0273(02)00241-X.
Scheuber, E., Giese, P., 1999. Architecture of the Central Andes - a compilation of geoscientific data along a transect at 21°S. J. S. Am. Earth Sci. 12 (2):103–107. https://doi.org/10.1016/S0895-9811(99)00008-5.
Shea, T., van Wyk de Vries, B., Pilato, M., 2008. Emplacement mechanisms of contrasting debris avalanches at Volcán Mombacho (Nicaragua), provided by structural and facies analysis. Bull. Volcanol. 70:899. https://doi.org/10.1007/s00445-007-0177-7.
Siebert, L., 1984. Large volcanic debris avalanches: characteristics of source areas, deposits, and associated eruptions. J. Volcanol. Geotherm. Res. 22 (3–4):163–197. https://doi.org/10.1016/0377-0273(84)90002-7.
de Silva, S.L., Self, S., Francis, P.W., Drake, R.E., Ramírez, C., 1994. Effusive silicic volcanism in the Central Andes: the Chao dacite and other young lavas of the Altiplano-Puna volcanic complex. J. Geophys. Res. 99 (B9):17805. https://doi.org/10.1029/94JB00652.
Sparks, R.S.J., Folkes, C.B., Humphreys, M.C.S., Barfod, D.N., Clavero, J., Sunagua, M.C., McNutt, S.R., Prichtard, M.E., 2008. Uturuncu Volcano, Bolivia: volcanic unrest due to midcrustal magma intrusion. Am. J. Sci. 308 (6):727–769. https://doi.org/10.2475/06.2008.01.
Takarada, S., Ui, T., Yamamoto, Y., 1999. Depositional features and transportation mechanism of valley-filling Iwasegawa and Kaida debris avalanche, Japan. Bull. Volcanol. 60 (7):508–522. https://doi.org/10.1007/s004450050248.
Tassi, F., Aguilera, F., Darrah, T., Vaselli, O., Capaccioni, B., Poreda, R.J., Delgado-Huertas, A., 2010. Fluid geochemistry of hydrothermal systems in the Arica-Parinacota, Tarapacá and Antofagasta regions (northern Chile). J. Volcanol. Geotherm. Res. 192 (1–2): 1–15. https://doi.org/10.1016/j.jvolgeores.2010.02.006.
Thouret, J.-C., Rivera, M., Wörner, G., Gerbe, M.-C., Finizola, A., Fornari, M., González, K., 2005. Ubinas: the evolution of the historically most active volcano in southern Peru. Bull. Volcanol. 67 (6):557–589. https://doi.org/10.1007/s00445-004-0396-0.
Tibaldi, A., Corazzato, C., Rovida, A., 2009. Miocene-Quaternary structural evolution of the Uyuni-Atacama región, Andes of Chile and Bolivia. Tectonophysics 471 (1–2): 114–135. https://doi.org/10.1016/j.tecto.2008.09.011.
Tierney, C.R., Schmitt, A.K., Lovera, O.M., de Silva, S.L., 2016. Voluminous plutonism during volcanic quiescence revealed by thermochemical modeling of zircon. Geology 44 (8): 683–686. https://doi.org/10.1130/G37968.1.
Trumbull, R., Riller, U., Oncken, O., Scheuber, E., Munier, K., Hongn, F., 2006. The timespace distribution of cenozoic volcanism in the South-Central Andes: a new data compilation and some tectonic implications. In: Oncken, O., Chong, G., Franz, G., Giese, P., Götze, H.-J., Ramos, V.A., Strecker, M.R., Wigger, P. (Eds.), The Andes: Active Subduction Orogeny, Frontiers in Earth Sciences, 1: 29–43. Springer, Heidelberg, Berlin, Germany. https://doi.org/10.1007/978-3-540-48684-8_2.
Ui, T., 1983. Volcanic dry avalanche deposits – identification and comparison with non-volcanic debris stream deposits. J. Volcanol. Geotherm. Res. 18 (1–4):135–150. https://doi.org/10.1016/0377-0273(83)90006-9.
Ui, T., 1989. Discrimination between debris avalanches and other volcaniclastic deposits. In: Latter, J.H. (Ed.), Volcanic Hazards: Assessment and Monitoring. Springer, Heidelberg, Berlin, Germany:pp. 201–209 https://doi.org/10.1007/978-3-642-73759-6_13.
Ui, T., Kawachi, S., Neall, V.E., 1986. Fragmentation of debris avalanche material during flowage – evidence from the Pungarehu Formation, Mount Egmont, New Zealand. J. Volcanol. Geotherm. Res. 27 (3–4):255–264. https://doi.org/10.1016/0377-0273(86)90016-8.
Ui, T., Takarada, S., Yoshimoto, M., 2000. Debris avalanches. In: Sigurdsson, H., Houghton, B., Rymer, H., Stix, J., McNutt, S. (Eds.), Encyclopedia of Volcanoes, First edition Academic Press, San Diego, CA, USA, pp. 617–626.
Urzua, L., Powell, T., Cumming, W., Dobson, P., 2002. Apacheta, a new geothermal prospect in Northern Chile. Geotherm. Res. Council Trans. 26, 65–69.
Valderrama, P., Roche, O., Samaniego, P., van Wyk de Vries, B., Bernerd, K., Mariño, J., 2016. Dynamic implications of ridges on a debris avalanche deposit at Tutupaca volcano (southern Peru). Bull. Volcanol. 78:14. https://doi.org/10.1007/s00445-016-1011-x.
Voight, B., 2000. Structural stability of andesite volcanoes and lava domes. Philos. Trans. R. Soc. Lond. A 358:1663–1703. https://doi.org/10.1098/rsta.2000.0609.
Voight, B., Glicken, H., Janda, R.J., Douglass, P.M., Lipman, P.W.Y., Mullineaux, D.R., 1981. Catastrophic rockslide avalanche of May 18. The 1980 Eruptions of Mount St. Helens, Washington. U.S. Geol. Surv. Prof. Pap. 1250, pp. 347–377.
Voight, B., Komorowsi, J.-C., Norton, G.E., Belousov, A.B., Belousova, M., Boudon, G., Francis, P.W., Franz, W., Heinrich, P., Sparks, R.S., Young, S.R., 2002. The 26 December (Boxing Day) 1997 sector collapse and debris avalanche at Soufrière Hills Volcano, Montserrat. In: Druitt, T.H., Kokelaar, B.P. (Eds.), The Eruption of Soufrière Hills Volcano, Montserrat, from 1995 to 1999. Geological Society, London, Memories 21: pp. 363–407. https://doi.org/10.1144/GSL.MEM.2002.021.01.17.
Wadge, G., Francis, P.W., Ramirez, C.F., 1995. The Socompa collapse and avalanche event. J. Volcanol. Geotherm. Res. 66 (1–4):309–336. https://doi.org/10.1016/0377-0273(94)00083-S.
Wooller, L., van Wyk de Vries, B., Cecchi, E., Rymer, H., 2009. Analogue models of the effect of long-term basement fault movement on volcanic edifices. Bull. Volcanol. 71 (10): 1111–1131. https://doi.org/10.1007/s00445-009-0289-3.
van Wyk de Vries, B., Delcamp, A., 2015. Volcanic debris avalanches. In: Davies, T., Shroder Jr., J.F. (Eds.), Landslide Hazards, Risks and Disasters. Elsevier Inc.:pp. 131–157 https://doi.org/10.1016/B978-0-12-396452-6.00005-7.
van Wyk de Vries, B., Francis, P.W., 1997. Catastrophic collapse at stratovolcanoes induced by gradual volcano spreading. Nature 387 (6631):387–390. https://doi.org/10.1038/387387a0.
van Wyk de Vries, B., Kerle, N., Petley, D., 2000. Sector collapse forming at Casita volcano, Nicaragua. Geology 28 (2):167–170. https://doi.org/10.1130/0091-7613.
van Wyk de Vries, B., Self, S., Francis, P.W., Keszthelyi, L., 2001. A gravitational spreading origin for the Socompa debris avalanche. J. Volcanol. Geotherm. Res. 105 (3): 225–247. https://doi.org/10.1016/S0377-0273(00)00252-3.